Chapter 22
Characterization of the Dynamical Model of a Force Sensor for Robot Manipulators

Ezio Bassi, Francesco Benzi, Luca Massimiliano Capisani, Davide Cuppone, and Antonella Ferrara

22.1 Introduction

Recent advances in robotics include the capability of planning a suitable trajectory in order to drive the robot from an initial configuration to a pre-determined goal point, or to follow, when possible, a pre-specified trajectory even in unknown environments [8]. Various methods can be adopted to accomplish this task. These methods are mainly classified in relation to the capability of the sensors which are employed to map the environment and the obstacles near the robot. When distance sensors and cameras are considered, the trajectory can be planned without colliding with the obstacles (i.e. no force measurements are required), see [3, 12, 13].

In contrast, considering only force sensors, the robot must collide with the obstacles in order to detect their presence and location and to plan a suitable trajectory to reach the goal [6, 7, 11, 18]. In this case, it is fundamental to design a suitable control law to reduce the risk of harming the robot or the obstacles themselves. Moreover, the use of force sensor is advisable in many position/force control schemes for robot manipulators. In all the mentioned cases, it is important to formulate an accurate model of the sensor to correctly measure the relevant contact forces.

In this paper, a case is considered in which a force sensor is mounted on the end-effector of a robot manipulator. The force revealed by the sensor results not only from the actual contact force between the tip of the sensor and the environment, but also from other dynamical effects, related to gravity, centripetal and Coriolis forces, accelerations of the tip of the sensor, and noise due to vibrations or electrical disturbances (see [14]). To determine reliable force measurements, it is necessary

Ezio Bassi, Francesco Benzi, and Davide Cuppone
Department of Electrical Engineering, University of Pavia, via A. Ferrata 1, Pavia 27100, Italy, e-mail: {ezio.bassi,fbenzi}@unipv.it,da.cuppone@gmail.com

Luca M. Capisani and Antonella Ferrara
Department of Computer Engineering and Systems Science, University of Pavia, via A. Ferrata 1, Pavia 27100, Italy, e-mail: {luca.capisani,antonella.ferrara}@unipv.it

to estimate the dynamical effects which generate forces not related with the actual contact forces, so as to eliminate these effects from the measured force.

In this work, a planar manipulator in the vertical plane is considered. Starting from the manipulator kinematics, a dynamical model of the sensor and its tip is formulated. Then, identification experiments to estimate the unknown parameters of the sensor and tip dynamical model are designed. The presented identification procedure is oriented to minimize the noise effects on the estimate, by choosing parametrized experiments which are optimized considering a scalar valued information function of the collected data [16, 17]. To deal with input noise, the approach proposed by [19] has been followed. This approach consists in repeating the same optimized experiment many times. In this way, assuming Gaussian input noise, it is possible to determine an estimation of the average input and average output signals, reducing the noise effects.

The model is then used to make the sensor measurements more accurate. Finally, it is analyzed how to obtain the absolute value and the direction of the contact force. Note that by enhancing the quality of the force measurements, the application of robust position controllers provides improved performances (e.g., see [2, 5, 9]).

The identification experiment, made on a COMAU SMART3-S2 anthropomorphic rigid robot manipulator with an ATI Gamma force sensor, is finally described.

22.2 Sensor Measurements

A fundamental part of a force control loop is the determination of the contact force between the tip of the manipulator and the environment [18]. The considered force sensor measures the force f acting on its tip. This force is described in the $O-xy$ vertical plane indicated in Fig. 22.1, which represents the manipulator workspace. The force f is composed by two terms

$$f = \begin{bmatrix} f_x & f_y & \tau_z \end{bmatrix}^T = f_0 + f_c, \qquad f_c = \begin{bmatrix} f_{cx} & f_{cy} & \tau_{cz} \end{bmatrix}^T \tag{22.1}$$

where f_0 refers to the forces related to the tip dynamics and f_c refers to the forces related to the contact with the environment. Vector f contains the force and the torque generated because of the contact, and the dynamical effects on the sensor tip, where f_x and f_y are the components of the force and τ_z is the corresponding torque revealed by the sensor. The torque τ_{cz} on P_s is generated by the forces f_{cx} and f_{cy}.

The objective is to determine a suitable model in order to eliminate the effect of f_0 in (22.1), so that the remnant force is actually the contact force. This implies that if the tip is not in contact with the environment, the considered force has to be zero.

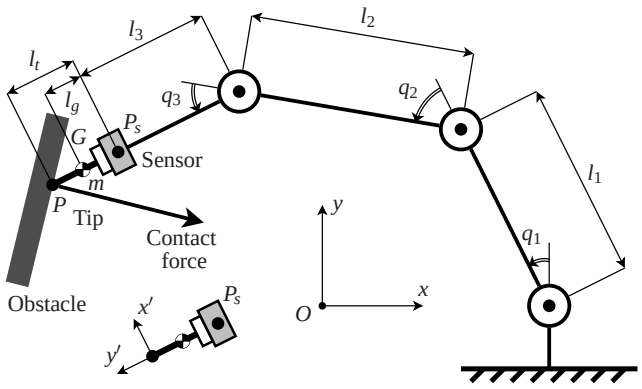

Fig. 22.1 Three link planar manipulator

22.3 The Kinematic Model of the Robot

To analyze the dynamical effects of the masses of the sensor and the tip which determine the term f_0 in (22.1), it is necessary to introduce the kinematic model of the robot.

In this paper, only vertical planar motions are considered, by locking three of the six joints of the manipulator (note that the extension to the spatial motions is possible, but in this case the dynamic model of the tip is more complicated). The kinematic model describes the relation between the configuration $q = [q_1, q_2, q_3]^T$ of the three considered joints and the end-effector position and orientation $P = [P_x, P_y, \phi]^T$ in the vertical plane $\{x,y\}$ which is the workspace. The angular term q_1 is the orientation of the first link with respect to the y axis clockwise positive, while $q_j,\ j = 2,3$, define the displacement of the $j-th$ link with respect to the $(j-1)-th$, clockwise positive (see Fig. 22.1).

The first rotational joint of the manipulator is located at the origin O of the $\{x,y\}$ plane. The position of the sensor and of the extreme point of the robot are

$$P_s = \sum_{k=1}^{3} \begin{bmatrix} l_k \sin(\sum_{z=1}^{k} q_z) \\ l_k \cos(\sum_{z=1}^{k} q_z) \end{bmatrix}, \qquad P = P_s + l_t \begin{bmatrix} \sin(q_1+q_2+q_3) \\ \cos(q_1+q_2+q_3) \end{bmatrix} \tag{22.2}$$

where q_i and l_i are the angular displacement and the length of the i-th link, respectively while l_t is the length of the tip. As indicated in Fig. 22.1, the point P is the extremal point of the tip of the end-effector, while the orientation of the tip with respect to the y axis is given by $\phi = q_1 + q_2 + q_3$. The position P_s of the sensor is given in the $\{x,y\}$ plane.

Now consider the center of gravity G of the rigid body given by the sensor and its tip (see Fig. 22.1). The position of the point G and its velocity v_G are given by

$$G = P_s + l_g \begin{bmatrix} \sin(\phi) \\ \cos(\phi) \end{bmatrix}, \qquad v_G = \dot{P}_s + l_g \begin{bmatrix} \dot{\phi}\cos(\phi) \\ -\dot{\phi}\sin(\phi) \end{bmatrix} \tag{22.3}$$

where l_g is the distance between G and the position of the force sensor P_s, m is the total mass of the tip and the sensor, which causes the forces that are measured by the sensor itself. Note that l_g and m are unknown. Then, the acceleration a_G is

$$a_G = \ddot{P}_s + l_g \begin{bmatrix} -\dot{\phi}^2 \sin(\phi) + \ddot{\phi} \cos(\phi) \\ -\dot{\phi}^2 \cos(\phi) - \ddot{\phi} \sin(\phi) \end{bmatrix} = \begin{bmatrix} a_{Gx} \\ a_{Gy} \end{bmatrix}. \tag{22.4}$$

Note that the the angular rotation of the tip with respect to the x axis is described by ϕ, and the angular velocity of the tip is given by $\dot{\phi} e_z$, where e_z is the unit vector in the z direction, normal to $\{x,y\}$. The angular acceleration is given by $\ddot{\phi} e_z$.

22.4 Sensor and Tip Dynamical Model

The dynamical model we have formulated is a relationship between the quantities which characterize the motion of the tip of the sensor and the forces generated and measured from the sensor itself. Note that in this paper it is assumed that the sensor is composed of two parts: the first part is fastened with the robot and its mass cannot produce forces measurable by the sensor since it can be viewed as a part of the link, while the second part is fastened with the tip, and its mass, jointly with the mass of the tip, can produce significant dynamical effects which can be revealed by the sensor. For this reason, the robot and the first part of the sensor are not considered in the formulation of the dynamical model. Only the structure composed by the tip and by the second part of the sensor is relevant for our analysis.

By relying on (22.4) and on the transport theorem [1], it is possible to express f_0', which is obtained by describing f_0 in the rotated $\{x',y'\}$ reference, as follows

$$f_0' = \begin{bmatrix} f_{0x'} \\ f_{0y'} \\ \tau_{0z} \end{bmatrix} = \begin{bmatrix} \bar{f}_{0x'} - m a_{Gx'} - mg \sin\phi \\ \bar{f}_{0y'} - m a_{Gy'} - mg \cos\phi \\ \bar{\tau}_{0z} - I\ddot{\phi} + m l_g (a_{Gx'} + g) \sin\phi \end{bmatrix} \tag{22.5}$$

where $g = 9.806$ m/s^2, I is the inertia of the sensor tip, which is unknown, and the terms $\bar{f}_{0x'}$, $\bar{f}_{0y'}$, $\bar{\tau}_{0z}$ take in account the unknown constant biases always present on the acquired generalized force.

Note that model (22.5) neglects some aspects as elasticity in transmissions and mechanical plays, which can affect the determination of G and ϕ, as well as their derivatives. Moreover, noise is present in the analog communication between the sensor and the dsPIC sampler. This is the reason why in the proposed identification procedure, suitable actions has been done to counteract biasing due to these unmodelled aspects. The procedure consists of the following steps: data sampling; model parametrization; trajectory optimization; execution of the optimized experiment for N^{exp} times (see [19]); determination of the average values for the input and the output signals; construction of a single identification input matrix, which will be denoted with $\Phi(\cdot)$, collecting all averaged input samples; determination of

a suitable preconditioner for the normal equations matrix, i.e., $\Phi(\cdot)^T\Phi(\cdot)$, see [4]; determination of the parameter vector θ^{LS} on the basis of the LS estimator [15]; validation of the identified model.

In the sequel, we will denote with the term *sample* of the optimized experiment $\mathscr{E}$ the set of the entries of two vectors: the first vector has, as components, the forces and the torques acquired, i.e. $y_i^{\mathscr{E}} = [f_{0x'i}^{\mathscr{E}}, f_{0y'i}^{\mathscr{E}}, \tau_{0zi}^{\mathscr{E}}]^T$, while the second has, as components, the parameters of the motion of the tip of the sensor: $u_i^{\mathscr{E}} = [\ddot{P}_{si}^{\mathscr{E}}, \phi_i^{\mathscr{E}}, \dot{\phi}_i^{\mathscr{E}}, \ddot{\phi}_i^{\mathscr{E}}]^T$. Each sample $s_i^{T\mathscr{E}} = [u_i^{T\mathscr{E}}, y_i^{T\mathscr{E}}]$ represents the inputs and outputs values at the discrete time instant i. At the end of an optimized experiment, an output vector $Y^{\mathscr{E}} = [y_1^{T\mathscr{E}}, ..., y_i^{T\mathscr{E}}, ..., y_{N^{\mathscr{E}}}^{T\mathscr{E}}]^T$, where $N^{\mathscr{E}}$ is the number of sampled data of the optimized experiment $\mathscr{E}$, and an input matrix $\Phi^{\mathscr{E}}(\cdot)$, which is a nonlinear function of all the input signals $u_i^{\mathscr{E}}$ and of their first and second time derivatives, are determined.

As for model parametrization, it is apparent that model (22.5) is linear in the parameters vector

$$\theta^o = [\bar{f}_{0x'}, \bar{f}_{0y'}, \bar{\tau}_{0z}, m, ml_g, I]^T \tag{22.6}$$

which contains the actual but unknown parameters. Therefore, the model can be rewritten in the parametrized linear form $Y = \Phi\theta^o$ where Φ is a suitable matrix. When a particular optimized experiment $\mathscr{E}$ is executed, the noise is present on the outputs, i.e. the model becomes

$$Y^{\mathscr{E}} = \Phi^{\mathscr{E}}(\ddot{P}_s, \phi, \dot{\phi}, \ddot{\phi})\theta^o + V \tag{22.7}$$

and V is supposed to be Gaussian. $\Phi^{\mathscr{E}}(\cdot)$ collects the values of the input samples, i.e. $\Phi^{T\mathscr{E}} = [\Phi_1^{T\mathscr{E}}, \ldots, \Phi_i^{T\mathscr{E}}, \ldots, \Phi_N^{T\mathscr{E}}]$ and $\Phi_i^{T\mathscr{E}}$ is an input transformation at the time instant i,

$$\Phi_i^{\mathscr{E}} = \begin{bmatrix} 1 & 0 & 0 & M_{1i} & M_{2i} & 0 \\ 0 & 1 & 0 & M_{3i} & M_{4i} & 0 \\ 0 & 0 & 1 & 0 & M_{1i} & M_{2i} \end{bmatrix} \tag{22.8}$$

where M_{ki} refers to the value of $M_k(t)$ for the optimized experiment $\mathscr{E}$ at the time instant $t = iT$,

$$\begin{aligned} M_1 &= \left[\ddot{P}_{sx}\cos\phi - \left(\ddot{P}_{sy} + g\right)\sin\phi\right], \qquad M_2 = \ddot{\phi}, \\ M_3 &= -\left[\ddot{P}_{sx}\sin\phi + \left(\ddot{P}_{sy} + g\right)\cos\phi\right], \quad M_4 = \dot{\phi}^2. \end{aligned} \tag{22.9}$$

To design each optimized experiment, Finite Fourier Series have been considered

$$\begin{cases} q_1^r(t) = \sum_{i=1}^3 \left[x_i \sin\frac{2\pi it}{T} + x_{i+3}\cos\frac{2\pi it}{T} + x_{i+6}\sin\frac{2\pi(i+3)t}{T}\right] \\ q_2^r(t) = \sum_{i=1}^3 \left[x_i \sin\frac{2\pi it}{T} + x_{i+3}\cos\frac{2\pi it}{T} + x_{i+9}\sin\frac{2\pi(i+3)t}{T}\right] \\ q_3^r(t) = \sum_{i=1}^3 \left[x_i \sin\frac{2\pi it}{T} + x_{i+3}\cos\frac{2\pi it}{T} + x_{i+12}\sin\frac{2\pi(i+3)t}{T}\right] \end{cases} \tag{22.10}$$

where $x \in \mathbb{R}^{15}$, so as to define parametrized reference signals $q_j^r(t)$ for the manipulator joints which can be optimized by choosing the vector x.

The function $\mathscr{F}$ to be optimized is a measure of the information contained in the matrix $M = \Phi^T \Phi$ in the Loewner sense, see [16]. Among the possible criteria which can be considered for the function $\mathscr{F}$ the *D*-criterion has been choosen, i.e. $\mathscr{F} = \det(M)$ which has many interesting properties, such as the independence of the informativity of M from the trajectory parametrization. Hence, the best choice for the optimized experiment parametrization is given by

$$x^{opt} = \text{argmax}_x \det(M) \tag{22.11}$$

in which M is obtained by simulating the values of the input matrix Φ when the inputs are given from the equations (22.10) with the choice (22.11). It can be proved that, in this way, it is possible to minimize the variance of each parameter estimate. Note that in our case, the feasibility of the trajectory determinable relying on x^{opt} through (22.10) has been verified a posteriori. Another approach could be that of applying a constrained optimization method.

As described by [19], the optimized experiment is executed N^{exp} times, so as to reduce the noise acting on the input signal. Then, the identification data set $\mathscr{S}$ is obtained by averaging the sampled signals obtained during the repeated experiments, i.e. each sample $s_i^{\mathscr{E}}$ of each experiment is considered to determine the samples related to the identification data set $s_i^{\mathscr{S}}$

$$s_i^{\mathscr{S}} = \frac{\sum_{\forall \mathscr{E}} s_i^{\mathscr{E}}}{N^{exp}}. \tag{22.12}$$

The data set $s^{\mathscr{S}}$ is then considered to perform the parameter identification.

22.5 Estimation of the Contact Force

Once the parameters of the model for the f_0 term in (22.1) are estimated, it is possible to determine a better estimation of the contact force f_c by evaluating the term

$$\hat{f}_c = f - R(-\phi)\Phi(\ddot{P}_s, \phi, \dot{\phi}, \ddot{\phi})\theta^{LS} \tag{22.13}$$

where $\hat{f}_c$ is the estimation of f_c, $\Phi(\ddot{P}_s, \phi, \dot{\phi}, \ddot{\phi})$ is the nonlinear transformation of the inputs at the time instant i, θ^{LS} is the estimated parameters vector, and $R(-\phi)$ is a rotation in the $\{x,y\}$ plane.

Note that the objective is to estimate the absolute value and the direction of the contact force f_c, while in (22.13) three equations are present, hence the problem of estimating the contact force is overdetermined. Let us denote with R the absolute value of the contact force (φ is its direction, with respect to the y axis). In absence of noise and unmodelled effects, f_c is given by

$$f_c = [f_{cx},\, f_{cy},\, \tau_{cz}]^T = [-R\sin\varphi,\, -R\cos\varphi,\, -Rd\sin\varphi] \tag{22.14}$$

where $d = \|P - P_S\| = l_t$. In presence of noise and unmodelled effects, $\hat{f}_c$ differs from f_c. Then, (22.14) can be rewritten as

$$\hat{f}_c = J(\vartheta^o) + \varepsilon, \quad \vartheta^o = [R, \varphi]^T \tag{22.15}$$

in which $J(\cdot)$ represents the nonlinear model (22.14) and $\varepsilon \in \mathbb{R}^3$ is unknown. By minimizing the term $\varepsilon^T \varepsilon$ with respect to ϑ^o, one obtains

$$\varphi = \arctan\left[\frac{\hat{f}_{cx} - \hat{\tau}_{cz} d}{\hat{f}_{cy}(1 + d^2)}\right], \quad R = \left|\frac{(\hat{\tau}_{cz} d - \hat{f}_{cx})\sin\varphi - \hat{f}_{cy}\cos\varphi}{1 + d^2 \sin^2\varphi}\right|. \tag{22.16}$$

Fig. 22.2 The COMAU SMART3-S2 robot and the force sensor with its tip

22.6 Description of the Considered Robotic System

The COMAU SMART3-S2 industrial anthropomorphic rigid manipulator, located at the Department of Electrical Engineering of the University of Pavia, is shown in Fig. 22.2. It consists of six-DOF actuated by six brushless electric motors. Six 12-bit resolvers supply accurate angular position measurements.

Torque transmission is provided by reducers. As previously mentioned, in this paper, for the sake of simplicity, a three-DOF planar manipulator is considered (see Fig. 22.1). That is, for our purposes, joints 1, 4 and 6 of the robot have been locked so that only joints 2, 3 and 5 are used. Yet, the proposed approach can be easily extended to a n-joint robot. The three considered joints are numbered as $\{1, 2, 3\}$. The mechanical reducers associated with each motor have a gear ratio of (207, 60, 37), respectively. Thus the accuracy (in the worst case, i.e. taking into account the minor gear ratio equal to 37) is $360/(2^{12} \cdot 37)$, which is quite satisfactory. The considered robot is equipped with an ATI Gamma force sensor. The analog output of the sensor is acquired and sampled with a FLEX dsPIC micro-controller [10].

22.7 Experimental Results

In this section a comment is made on the results obtained in practice by applying the described procedure. Note that all the experiments devoted to the identification of the parameters of the sensor model are executed in the absence of contact forces f_c. In this case, the measures acquired during the experiments are due only because of the tracking of the trajectories and the gravity effect.

The optimization step performed to determine x^{opt} gives the following result, once the Matlab command *fminsearch* has been applied:

$$x^{opt} = \begin{matrix}[12.99,\ 8.95,\ -0.43,\ 5.72,\ 7.97,\ 11.42,\ 3.16,\ 1.92,\\ 9.49,\ -1.68,\ 4.40,\ 10.27,\ -1.33,\ 2.85,\ 2.01]^T\end{matrix}. \tag{22.17}$$

In this case, the value reached for the objective function is $\det(M) > 10^{41}$. The end of optimization procedure is reached after 115 evaluations of the objective function. Then, after the execution of the optimized experiments and the data averaging to determine the data related to the identification experiment, the following parameter vector is obtained after the identification step

$$\theta^{LS} = [15.0119\text{N},\ 0.2465\text{N},\ -1.3342\text{N},\ 0.2630\text{kg},\ 0.0127\text{kgm},\ 0.018\text{kgm}^2]^T. \tag{22.18}$$

The objective function determined considering the data set of the identification experiment is $\det(M^{\mathscr{S}}) > 10^{36}$.

Table 22.1 Identification and validation tests data sets residuals analysis

Data set	Mean Error			Variance σ^2		
	$E[\hat{f}_{0x'} - f_{0x'}]$ 10^{-13}[N]	$E[\hat{f}_{0y'} - f_{0y'}]$ 10^{-13}[N]	$E[\hat{\tau}_{0z} - \tau_{0z}]$ 10^{-13}[Nm]	$Var[\hat{f}_{0x'} - f_{0x'}]$ [N^2]	$Var[\hat{f}_{0y'} - f_{0y'}]$ [N^2]	$Var[\hat{\tau}_{0z} - \tau_{0z}]$ [N^{2}m^2]
$\mathscr{E} = 1$	-0.474	0.095	-0.017	0.819	2.207	0.002
$\mathscr{E} = 2$	-0.643	0.088	-0.042	0.469	3.435	0.029
$\mathscr{E} = 3$	-0.402	0.195	-0.009	0.672	2.170	0.008
$\mathscr{E} = 4$	-0.514	0.011	0.008	0.740	3.645	0.033
$\mathscr{E} = 5$	0.849	0.072	0.047	0.575	2.610	0.003
$\mathscr{E} = 6$	-0.488	0.040	0.004	0.697	2.516	0.002
$\mathscr{E} = 7$	0.439	-0.039	0.039	0.778	2.784	0.006
$\mathscr{E} = 8$	-0.438	0.091	0.029	0.658	2.320	0.007
$\mathscr{E} = 9$	-0.518	-0.067	-0.001	0.644	2.202	0.024
$\mathscr{E} = 10$	-0.386	0.104	-0.108	0.653	2.649	0.003
$\mathscr{S}$	0.465	-0.026	0.044	0.037	0.110	0.000
$\mathscr{V}$	0.005×10^{13}	0.287×10^{13}	-0.001×10^{13}	0.464	1.597	0.001

As described in Subsection 22.4, the force measurements are affected by unpredictable noise which is due to the presence of electromagnetic waves generated by the robot actuation system and by the power suppliers. Despite the presence of these

disturbances during the real tests, with the proposed identification method, it is possible to obtain satisfying results. Table 22.1 shows the analysis relative to 10 of the $N^{exp} = 30$ identification data sets compared with the data set considered to estimate the model parameters. As can be observed from the analysis, the data coming from the averaged data set $\mathscr{S}$ lead to more satisfactory results in terms of noise variance reduction (note that the mean error is very low, due to the fact that the data sets have been considered for the estimation procedure).

Table 22.1 also shows the validation data set analysis. The validation experiment is similar to the optimized identification one. As can be noted, the estimated mean for the residuals (first three columns) is greater than the identification one, but it is acceptable. The same comment applies to the variance analysis.

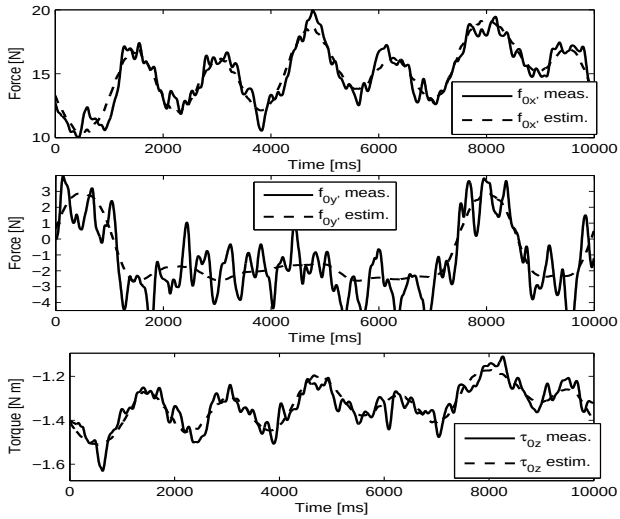

Fig. 22.3 Model validation: measurements and their prediction for the signals $f_{0x'}$, $f_{0y'}$, τ_{0z}

Fig. 22.3 shows the good performances of the model in validation. Moreover, it can be noted that the validation residuals are not comparable with the white noise. This effect is generated by the particular measurement strategy performed by the sensor, which is redundant in the sense that one can acquire three signals which describe a quantity, the force f_0, which has two degrees of freedom.

As can be observed in the second plot of Fig. 22.3, the less accurate estimation is obtained for the signal $f_{0y'}$. This is due to the low precision of the sensor in the y' direction. Yet, the two degrees of freedom force to be estimated is described by three signals, thus the scarcely accurate estimation of the $f_{0y'}$ signal is compensated by the other two estimations.

22.8 Conclusions

The paper considers the problem of determining reliable force measurements by compensating the dynamical effects which are present on the tip of a robot manipulator during the motion. A kinematic and a dynamic model are formulated starting from the manipulator structure. The parameters of the dynamic model are identified with the proposed identification procedure, which is designed so as to reduce the noise effects on the estimation and to optimize the information which can be captured during the identification experiments. Finally, a method to estimate the direction and the absolute value of the contact force is described. The identification and validation of experimental results obtained with the proposed identification procedure are quite satisfactory.

References

1. Biscari, P., Poggi, C., Virga, E.G.: Mechanics notebook. Liguori, Neaples, Italy (2005)
2. Calanca, A., Capisani, L.M., Ferrara, A., Magnani, L.: An inverse dynamics-based discrete-time sliding mode controller for robot manipulators. In K. Kozlowski, Editor. In: Robot Motion and Control 2007, pp. 137–146. Springer-Verlag, London, UK (2007)
3. Capisani, L.M., Facchinetti, T., Ferrara, A., Martinelli, A.: Environment modelling for the robust motion planning and control of planar rigid robot manipulators. In: Proc. 13th IEEE Conference on Emerging Technologies and Factory Automation, pp. 759–766. Hamburg, Germany (2008)
4. Capisani, L.M., Ferrara, A., Magnani, L.: MIMO identification with optimal experiment design for rigid robot manipulators. In: Proc. IEEE/ASME International Conference on Advanced Intelligent Mechatronics (2007)
5. Capisani, L.M., Ferrara, A., Magnani, L.: Design and experimental validation of a second order sliding-mode motion controller for robot manipulators. International Journal of Control **82**(2), 365–377 (2009)
6. Chiaverini, S., Sciavicco, L.: The parallel approach to force/position control of robotic manipulators. IEEE Transactions on Robotics and Automation **9**(4), 361–373 (1993)
7. Chiaverini, S., Siciliano, B., Villani, L.: Force/position regulation of compliant robot manipulators. IEEE Transactions on Automatic Control **39**(3), 647–652 (1994)
8. Choset, H., Lynch, K.M., Hutchinson, S., Kantor, G., Burgard, W., Kavraki, L.E., Thrun, S.: Principles of Robot Motion, Theory, Algorithms, and Implementations. MIT Press, Cambridge, Massachusetts, USA (2005)
9. Ferrara, A., Magnani, L.: Motion control of rigid robot manipulators via first and second order sliding modes. Journal of Intelligent and Robotic Systems **48**(1), 23–36 (2007)
10. Gai, P.: FLEX: Modular soultion for embedded applications. http://www.evidence.eu.com/download/manuals/pdf/flex_refman_1_0_ 1.pdf (2008)
11. Khatib, O.: Real-time obstacle avoidance for manipulators and mobile robots. The International Journal of Robotics Research **5**(1), 90–98 (1986)
12. Kim, J.O., Kosla, P.K.: Real-time obstacle avoidance using harmonic potential functions. IEEE Transactions on Robotics and Automation **8**(3), 338–349 (1992)
13. LaValle, S.M.: Planning algorithms. Cambridge University Press, Cambridge, Massachusetts, USA (2006)
14. Lee, S., Park, J., Kwon, T., Song, J.: Torque sensor calibration using virtual load for a manipulator. In: Proc. IEEE/RSJ International Conference on Intelligent Robots and Systems, pp. 2449–2454. San Diego, California, USA (2007)

15. Ljung, L.: System Identification - Theory for the user, 2nd edn. PTR Prentice Hall, New York, USA (1999)
16. Pukelsheim, F.: Optimal Design of Experiments. John Wiley & Sons, New York, USA (2006)
17. Rojas, C.R., Welsh, J.S., Goodwin, G.C., Feuer, A.: Robust optimal experiment design for system identification. Automatica **43**(6), 993–1008 (2007)
18. Siciliano, B., Sciavicco, L., Villani, L., Oriolo, G.: Robotics: Modelling, Planning and Control. Springer-Verlag, London, UK (2009)
19. Swevers, J., Verdonck, W., De Schutter, J.: Dynamic model identification for industrial robots. IEEE Control Systems Magazine **27**(5), 58–71 (2007)